

Reaction Dynamics – Molecular Spectroscopy

Andrew Orr-Ewing

School of Chemistry
University of Bristol, UK

www.bristoldynamics.com

Outline

1. Requirements of spectroscopic probes for reaction dynamics
2. Fundamentals of molecular spectroscopy
3. Spectroscopic techniques for reaction dynamics
 - Gas phase
 - Condensed phase
4. Two-dimensional spectroscopy
5. Simulation of spectra using PGOPHER

1.0 Requirements of spectroscopic probes of reaction dynamics

- **High sensitivity** – because of low densities in molecular beam experiments
- **Specificity** – to isolate signals from the molecules of interest
- **Quantum-state resolution** – for stringent tests of theory
- **High time resolution** – nanosecond to femtosecond to observe dynamics

Further desirable characteristics include measurement of **correlated properties**:

- Angular momentum polarization (alignment and orientation)
- Relative velocities and scattering angles, and dependence on quantum state
- Coherence and phase of quantum states, and dephasing times

1.1 Summary of spectroscopic techniques used in reaction dynamics

A. Gas phase / molecular beam experiments

- IR chemiluminescence
- Absorption spectroscopy (including Frequency Modulation Spectroscopy)
- **Laser Induced Fluorescence**
- **REMPI** and VUV ionization (combined with velocity map imaging, VMI)
- **Photoelectron spectroscopy** – Katharine Reid's lecture
- **Transient absorption spectroscopy**
- **XUV and X-ray absorption spectroscopy**
- Attosecond spectroscopy with HHG pulses – Valerie Blanchet's lecture

B. Condensed phase experiments

- **Transient absorption spectroscopy**
- Femtosecond stimulated Raman Spectroscopy
- **2D IR** and 2D electronic spectroscopy
- Time-resolved photoelectron spectroscopy with liquid jets

2.0 Fundamentals of molecular spectroscopy

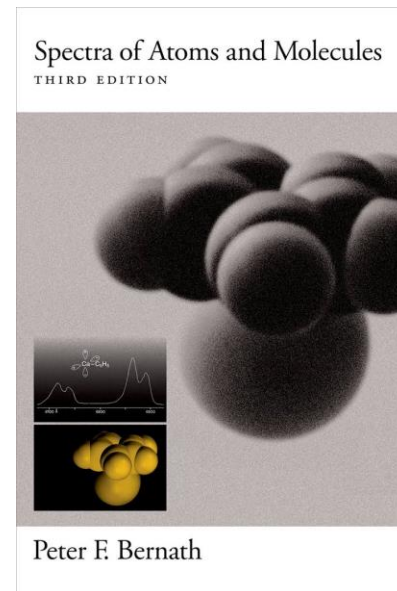
The spectroscopic methods probe rotational, vibrational and electronic energy levels (and parities) of molecules.

The patterns of these energy levels and the high-resolution spectroscopy of small molecules are discussed in numerous textbooks:

e.g. P.F. Bernath, *Spectra of Atoms and Molecules*

Focus here on:

- Transition dipole moments for molecules and symmetry constraints
- Multi-photon transitions and selection rules
- Spectroscopy of molecular ensembles: the density matrix picture for pump-probe and 2D spectroscopy



2.1 Transition dipole moments and absorption cross sections

The interaction of electromagnetic radiation with a molecule is treated using perturbation theory.

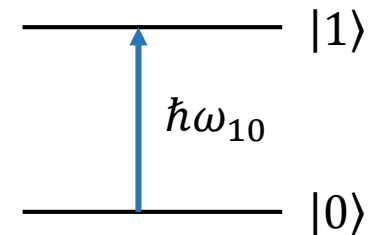
The electric-dipole interaction of the molecule with light is:

$$\hat{h}(t) = -\hat{\mu} \cdot \hat{E}(t) = -\hat{\mu} \cdot \hat{E}_0 \cos \omega t$$

With $\hat{\mu}$ denoting the electric dipole moment operator, and ω the frequency of the light.

The electric-dipole interaction can couple two states if

$$\langle 1 | \hat{\mu} \cdot \hat{E}(t) | 0 \rangle \neq 0$$



The absorption cross section $\sigma(\omega)$ is a measure of the strength of the transition and can be determined from the Beer-Lambert law:

$$\sigma(\omega) \propto |\langle 1 | \hat{\mu} \cdot \hat{E}_0 | 0 \rangle|^2 \propto |\langle 1 | \hat{\mu} | 0 \rangle \cdot \hat{E}_0|^2 \propto |\hat{\mu}_{10} \cdot \hat{E}_0|^2$$

$$\sigma(\omega) = \frac{\pi}{\hbar \epsilon_0 c} \omega_{10} \delta(\omega_{10} - \omega) |\langle 1 | \hat{\mu} \cdot \hat{E}_0 | 0 \rangle|^2$$

2.2 Selection rules

The dipolar interaction imposes some constraints on the absorption: spectroscopic selection rules, e.g. $\Delta J = 0, \pm 1$. For a transition to be allowed:

$$\hat{\mu}_{10} = \langle 1 | \hat{\mu} | 0 \rangle \neq 0$$

The product of the symmetries of $|1\rangle$ and $|0\rangle$ and $\hat{\mu}$ must be **totally symmetric**.

$$\Gamma_{|1\rangle} \otimes \Gamma_{\hat{\mu}} \otimes \Gamma_{|0\rangle} \supset A_1$$

e.g. symmetry of $\tilde{A}^1B_1 \leftarrow \tilde{X}^1A_1$ and $\tilde{B}^1A_1 \leftarrow \tilde{X}^1A_1$ bands of H_2O (C_{2v} symmetry)

C_{2v}	E	C_2	$\sigma_v(xz)$	$\sigma_v(yz)$	
A_1	1	1	1	1	z
A_2	1	1	-1	-1	
B_1	1	-1	1	-1	x
B_2	1	-1	-1	1	y

C_{2v}	A_1	A_2	B_1	B_2
A_1	A_1	A_2	B_1	B_2
A_2	A_2	A_1	B_2	B_1
B_1	B_1	B_2	A_1	A_2
B_2	B_2	B_1	A_2	A_1

$$B_1 \otimes B_1 \otimes A_1 = A_1$$

$$|1\rangle \quad \hat{\mu}_x \quad |0\rangle$$

2.3 Multiphoton transitions and selection rules

It is convenient to express the transition operator in spherical tensor form:

$T_q^k(\mu)$ k is the rank of the tensor
 q is the component (a projection quantum number with $|q| \leq k$)

Electric dipole transition: $k = 1, q = -1, 0, 1$

Two-photon transition: $k = 2, q = -2, -1, 0, 1, 2$ and $k = 0, q = 0$

For rotational wavefunctions $|JKM\rangle$ and with $|\eta\rangle$ denoting electronic and vibrational quantum numbers and states, the transition moments are:

$$\langle \eta' J' K' M' | T_q^k(\mu) | \eta J K M \rangle = (-1)^{J'-M'} \begin{pmatrix} J' & k & J \\ -M' & q & M \end{pmatrix} \times \\ \sum_p (-1)^{J'-K'} \sqrt{(2J'+1)(2J+1)} \begin{pmatrix} J' & k & J \\ -K' & p & K \end{pmatrix} \langle \eta' | T_p^k(\mu) | \eta \rangle$$

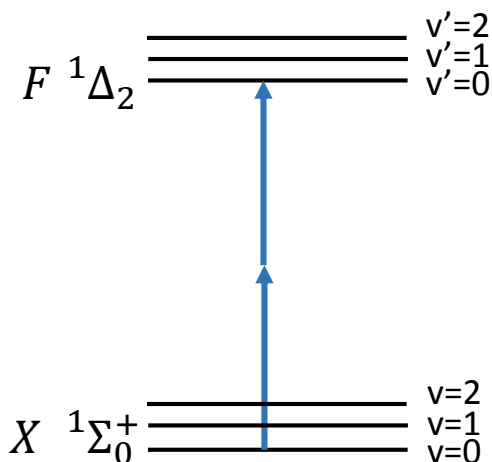
K is the body-fixed projection of J . Use Ω in a diatomic molecule.
 M is the space-fixed projection of J .

The Wigner 3-j symbols impose selection rules (in the body-fixed frame):

$$\begin{pmatrix} J' & k & J \\ -K' & p & K \end{pmatrix} = 0 \text{ unless } -K' + p + K = 0$$

$p = K' - K = \Delta K$, or $p = \Omega' - \Omega = \Delta\Omega$ for diatomic molecules.

e.g. The $F^1\Delta_2 - X^1\Sigma_0^+$ transition of HCl is allowed in a two-photon transition with a transition dipole moment operator $T_2^2(\mu)$.



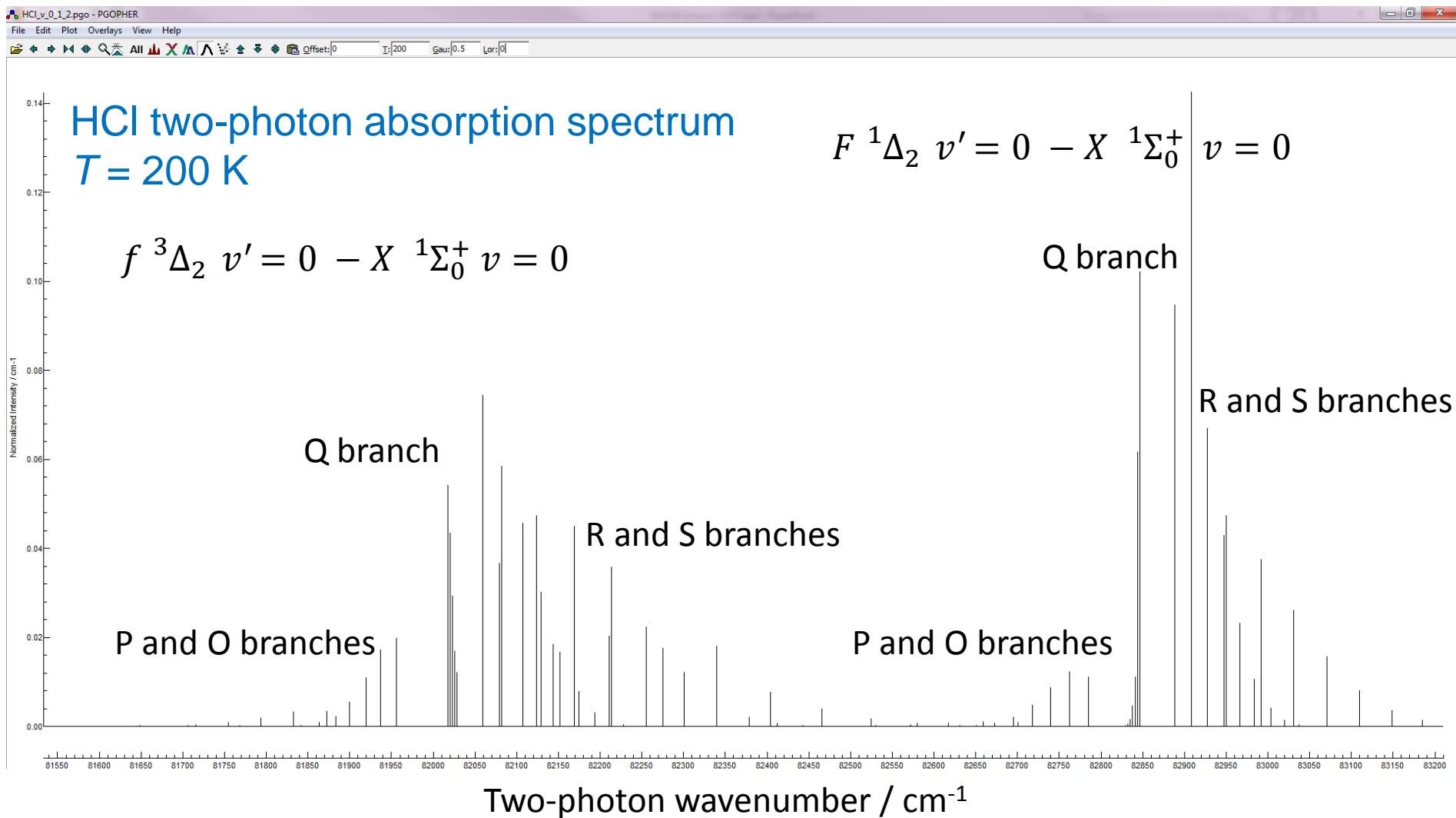
The PGOPHER simulation of the 2-photon $F^1\Delta_2 - X^1\Sigma_0^+$ transition uses matrix elements:

$$\langle F^1\Delta_2 v' = 0,1,2 | T_2^2(\mu) | X^1\Sigma_0^+ v = 0,1,2 \rangle$$

PGOPHER: A program for simulating rotational, vibrational and electronic spectra,
C.M. Western, J. Quant. Spectros. Radiat. Trans.
186, 221 (2017). <http://pgopher.chm.bris.ac.uk/>

For more detail on multiphoton selection rules see Ashfold *et al.* J. Chem. Soc. Faraday Trans. **89**, 1153 (1993)

Simulation of two-photon HCl spectrum using PGOPHER



$\Delta J = +2$	$\Delta J = +1$	$\Delta J = 0$	$\Delta J = -1$	$\Delta J = -2$
S branch	R branch	Q branch	P branch	O branch

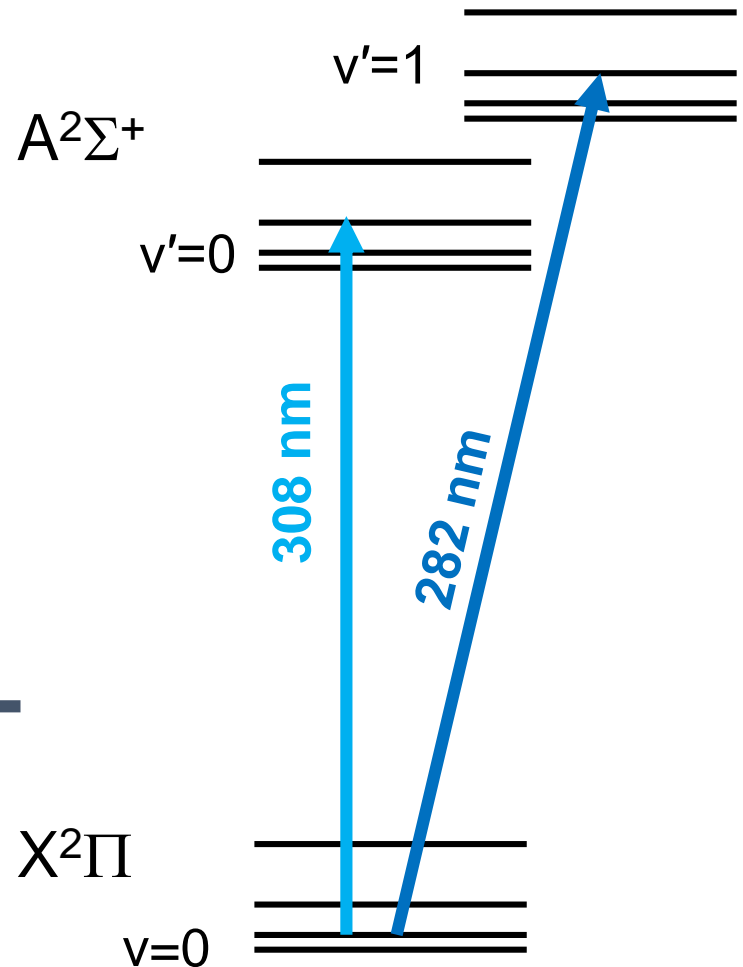
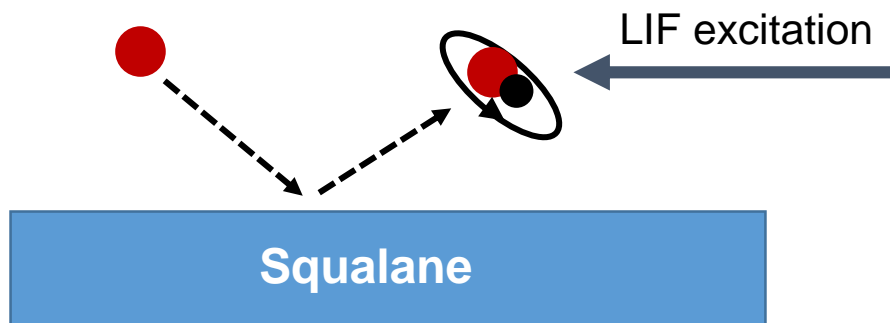
3.0 Spectroscopic techniques for reaction dynamics

3.1 Laser induced fluorescence (LIF) spectroscopy

Excite a one-photon transition in a molecule or radical (usually with nsec laser).

Image the fluorescence from an excited electronic state.

Common applications in chemical dynamics studies include detection of OH, e.g. in reactions of O(³P) at liquid hydrocarbon surfaces (K.G. McKendrick and coworkers).



Collect fluorescence from $A^2\Sigma^+$ state

3.2 Resonance Enhanced Multi-Photon Ionization (REMPI) spectroscopy

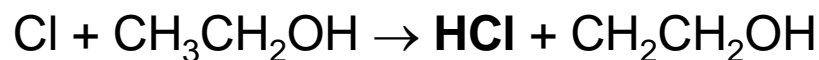
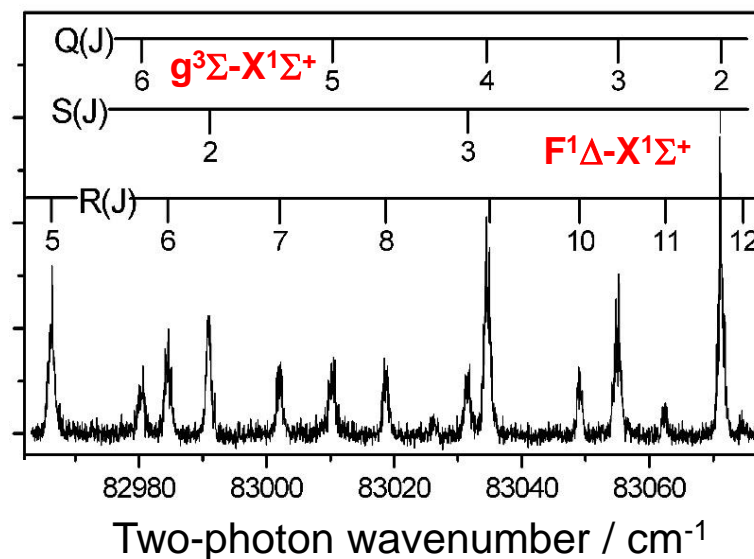
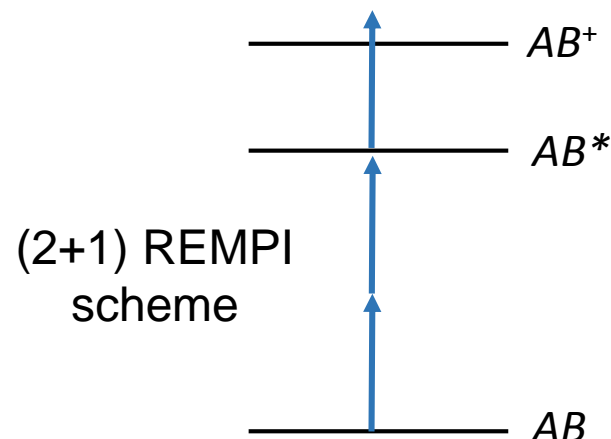
Use a focused, nanosecond laser pulse from a dye laser or OPO to excite an n photon absorption to a **Rydberg state** followed by an m photon absorption above the ionization limit.

$(n + m)$ REMPI spectroscopy.

Detect the resulting cations in a TOF mass spectrometer, often partnered with **velocity map imaging**.

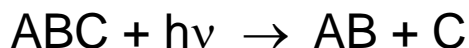
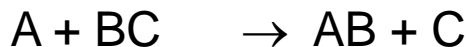
Convenient and popular (2+1) REMPI schemes for detection of H, Cl, Br, H₂, HCl, HBr, CH₃, NH₃, *etc.*

e.g. application in study of $\text{Cl} + \text{CH}_4 \rightarrow \text{HCl} + \text{CH}_3$ reaction (R.N. Zare, K. Liu, F.F. Crim, ...)

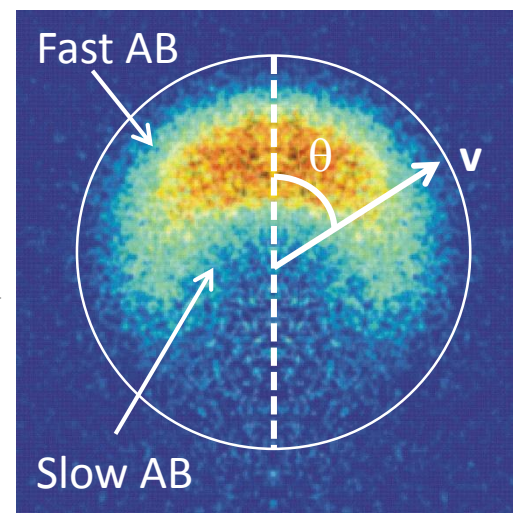
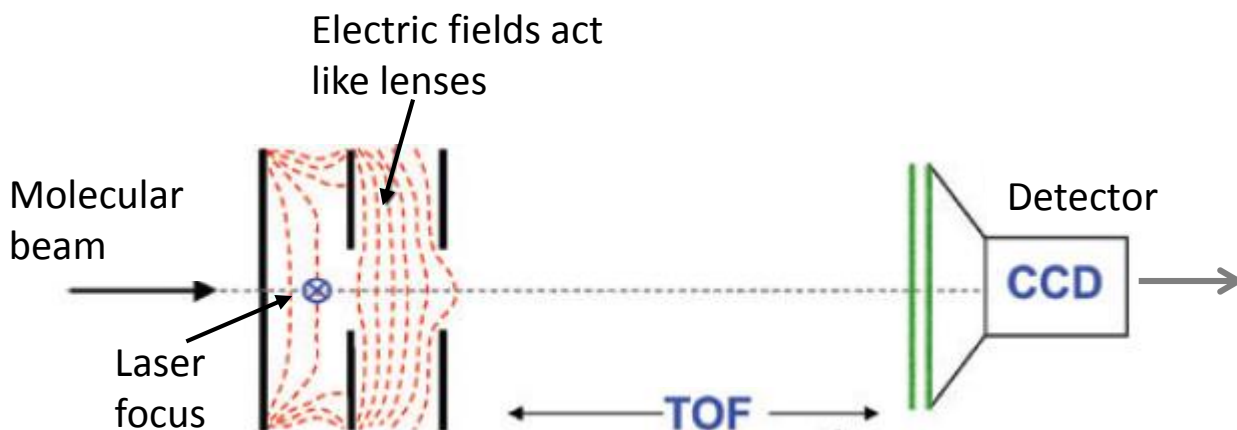


3.3 REMPI Spectroscopy and Velocity Map Imaging

Powerful combination to study photodissociation and reaction dynamics



- Use REMPI to ionize products of a chemical reaction (make AB^+)
- Use carefully designed electric fields to accelerate the ions to a detector
- Detector located at the end of a TOF mass spectrometer to give mass resolution
- Record where the AB^+ ions hit the detector using a CCD camera
- Point of impact on detector depends on initial velocity (speed and direction) of AB

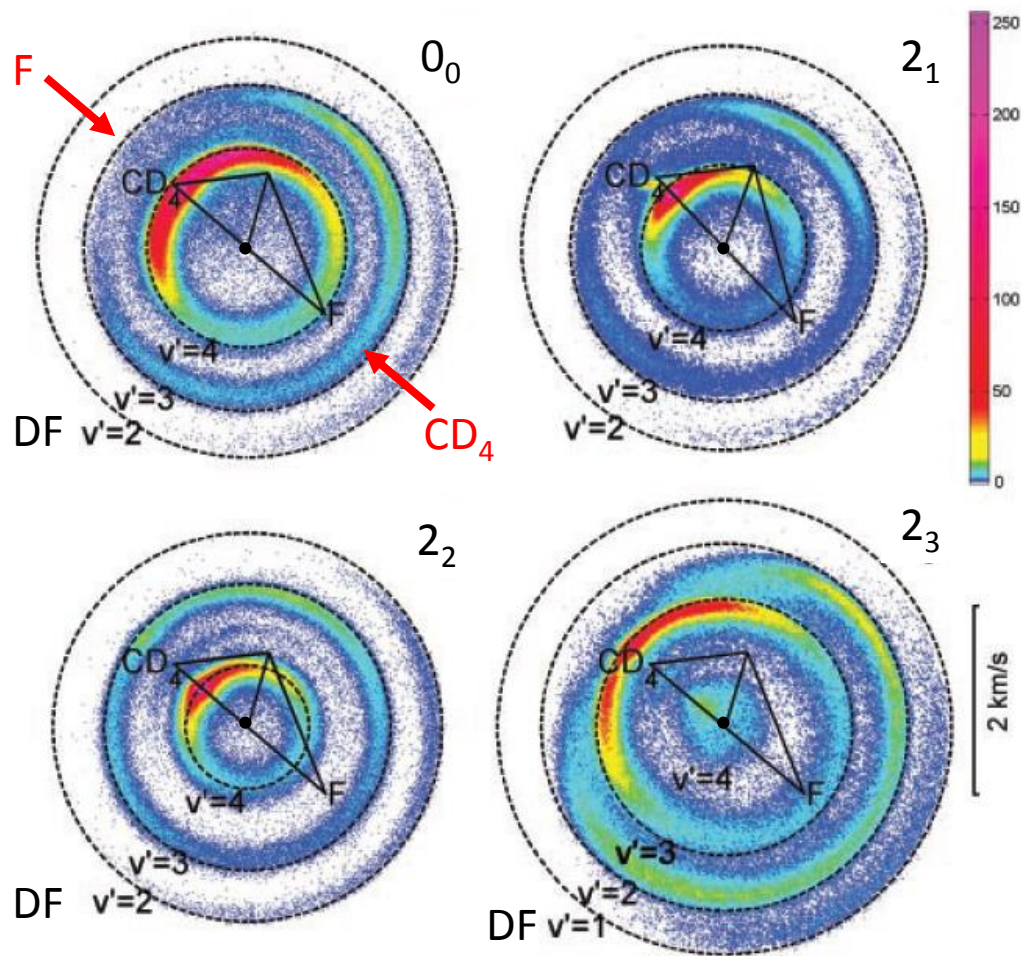
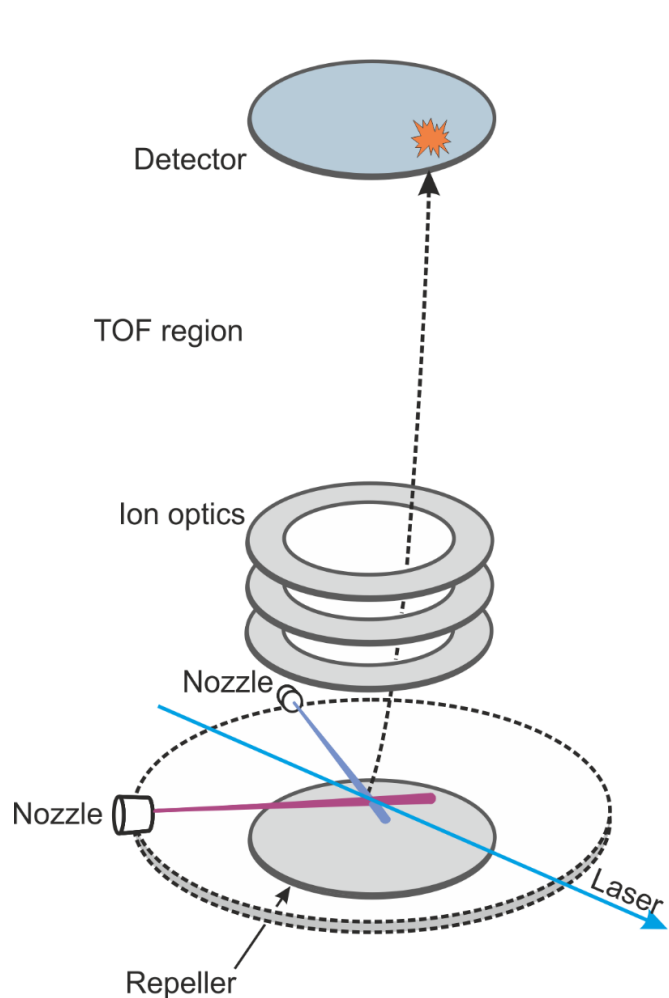


See Ashfold *et al.* PCCP **8**, 26 (2006) for a review

Each point corresponds to a particular v and θ

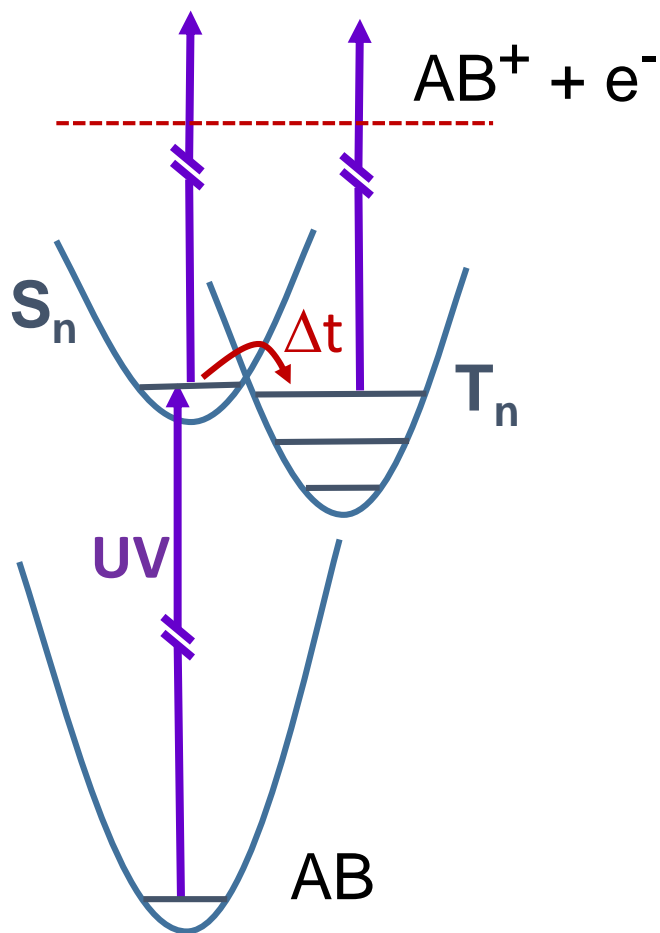
Example: VMI of $F + CD_4 \rightarrow DF(v) + CD_3$

- REMPI detection of CD_3 in umbrella modes $v_2 = 0, 1, 2, 3$ (denoted $2_0, 2_1, 2_2, 2_3$).
- Select quantum state of CD_3 by choice of laser wavelength for REMPI
- By energy conservation, slower $CD_3 \Rightarrow$ greater internal (vibrational) energy of DF



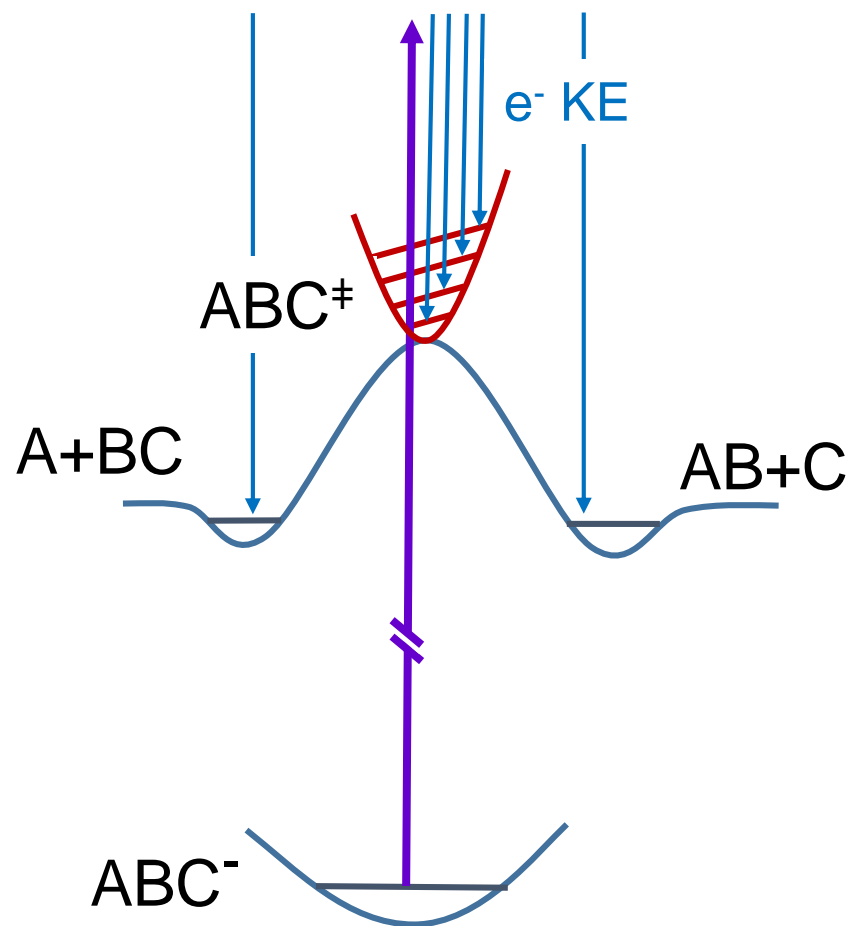
3.4 Photoelectron spectroscopy as a probe of chemical dynamics

Time-resolved photoelectron spectroscopy



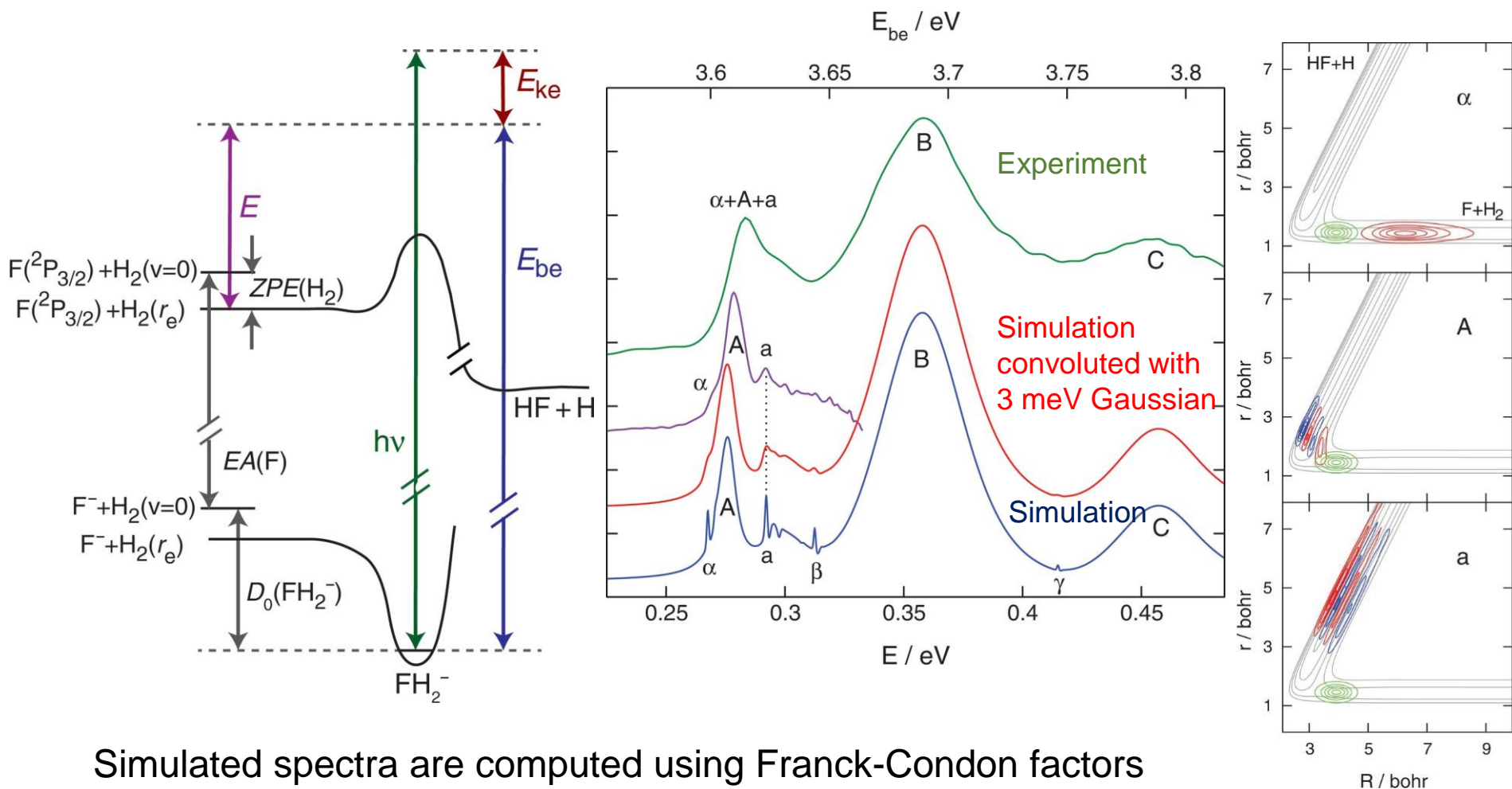
Stolow *et al.* Chem Rev. **104**, 1719 (2004)
Suzuki, Ann. Rev. Phys. Chem. **57**, 555 (2006)

Anion photodetachment



e.g., Kim *et al.*, Science **349**, 510 (2015)

Example: Anion photodetachment study of the F + H₂ reaction



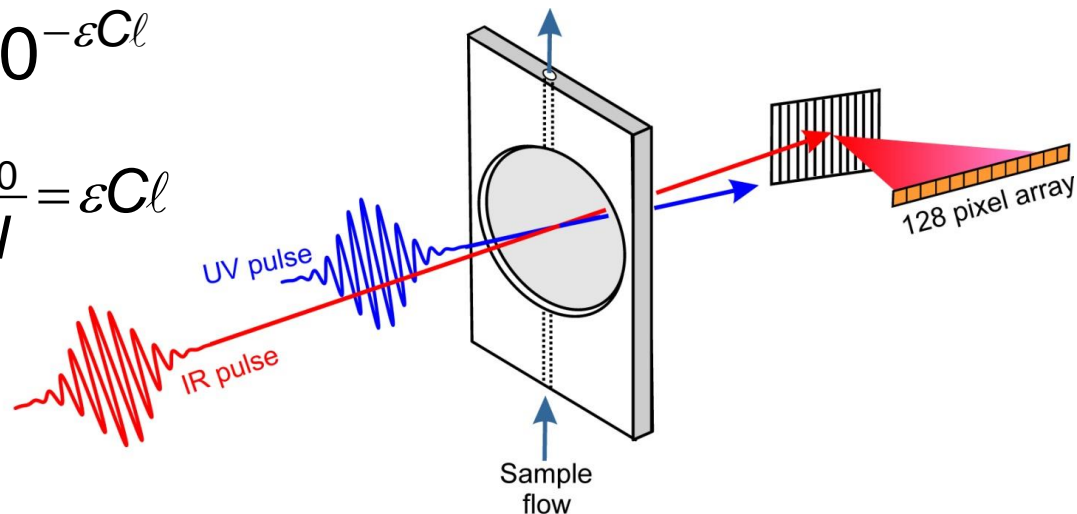
Simulated spectra are computed using Franck-Condon factors (assuming a constant electronic transition dipole matrix element):

$$P(E) = \langle \psi_{vib}(FH_2^-) | \psi_{scat}^E(FH_2) \rangle$$

3.5 Transient absorption spectroscopy

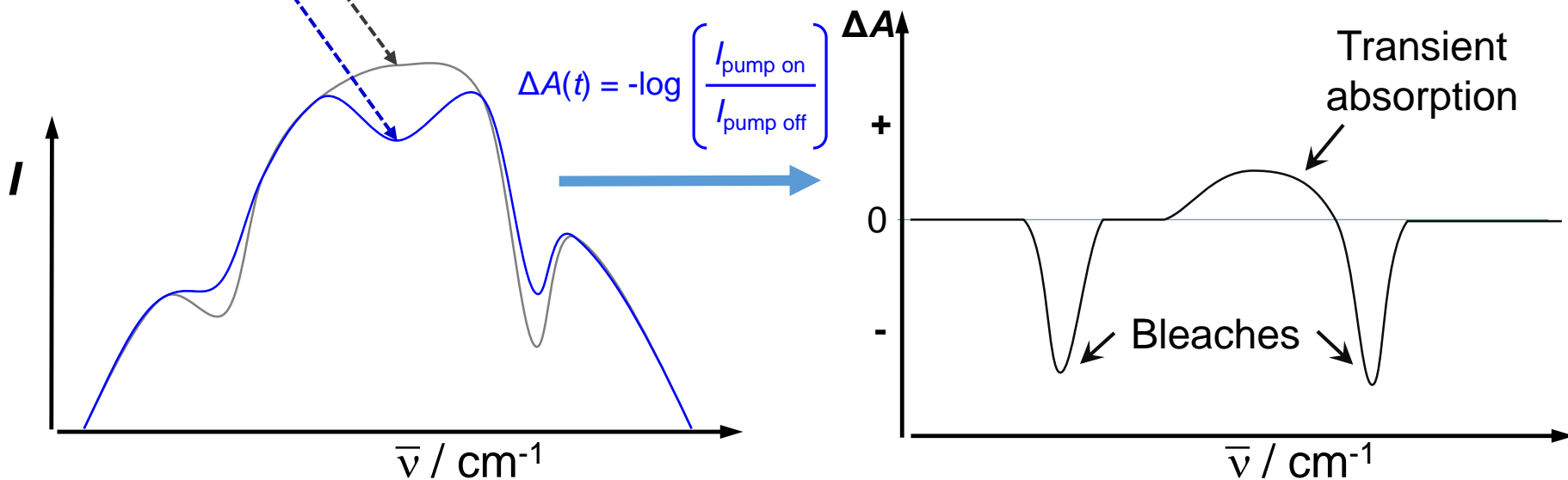
Beer-Lambert Law: $I = I_0 10^{-\epsilon C l}$

$$A = \log_{10} \frac{I_0}{I} = \epsilon C l$$



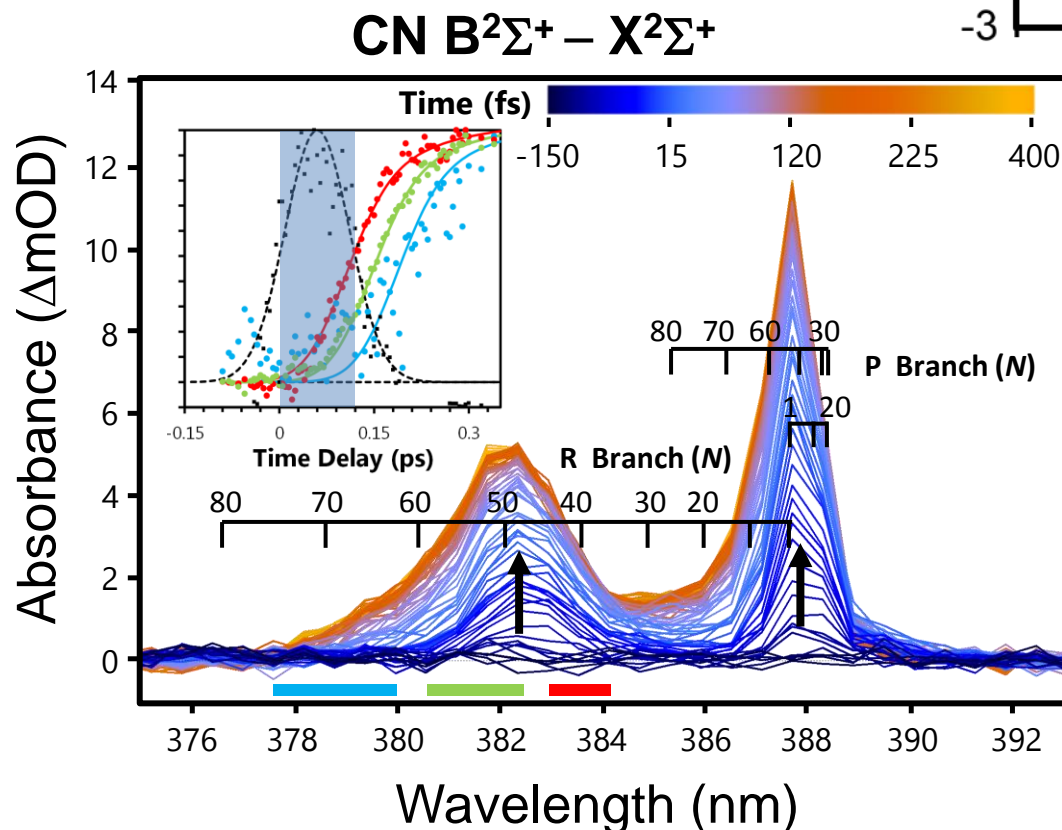
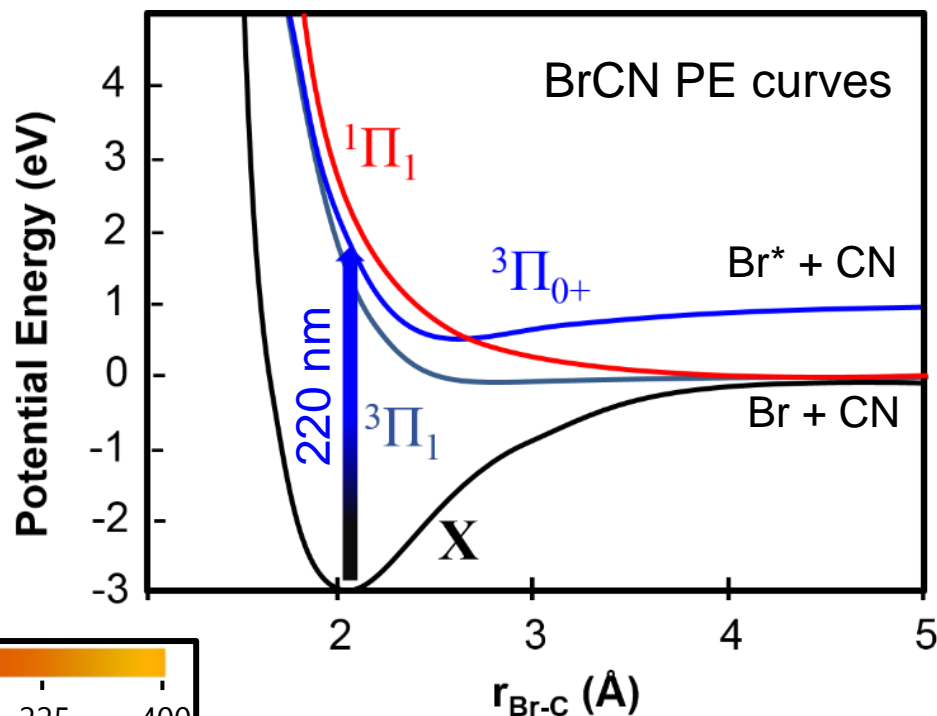
UV pulse off

UV pulse on



Example: Transient absorption spectroscopy of CN radicals from 220-nm photolysis of BrCN

CN radicals are produced highly rotationally excited ($N \sim 50$) because of angular anisotropy on the dissociative excited state PESs.

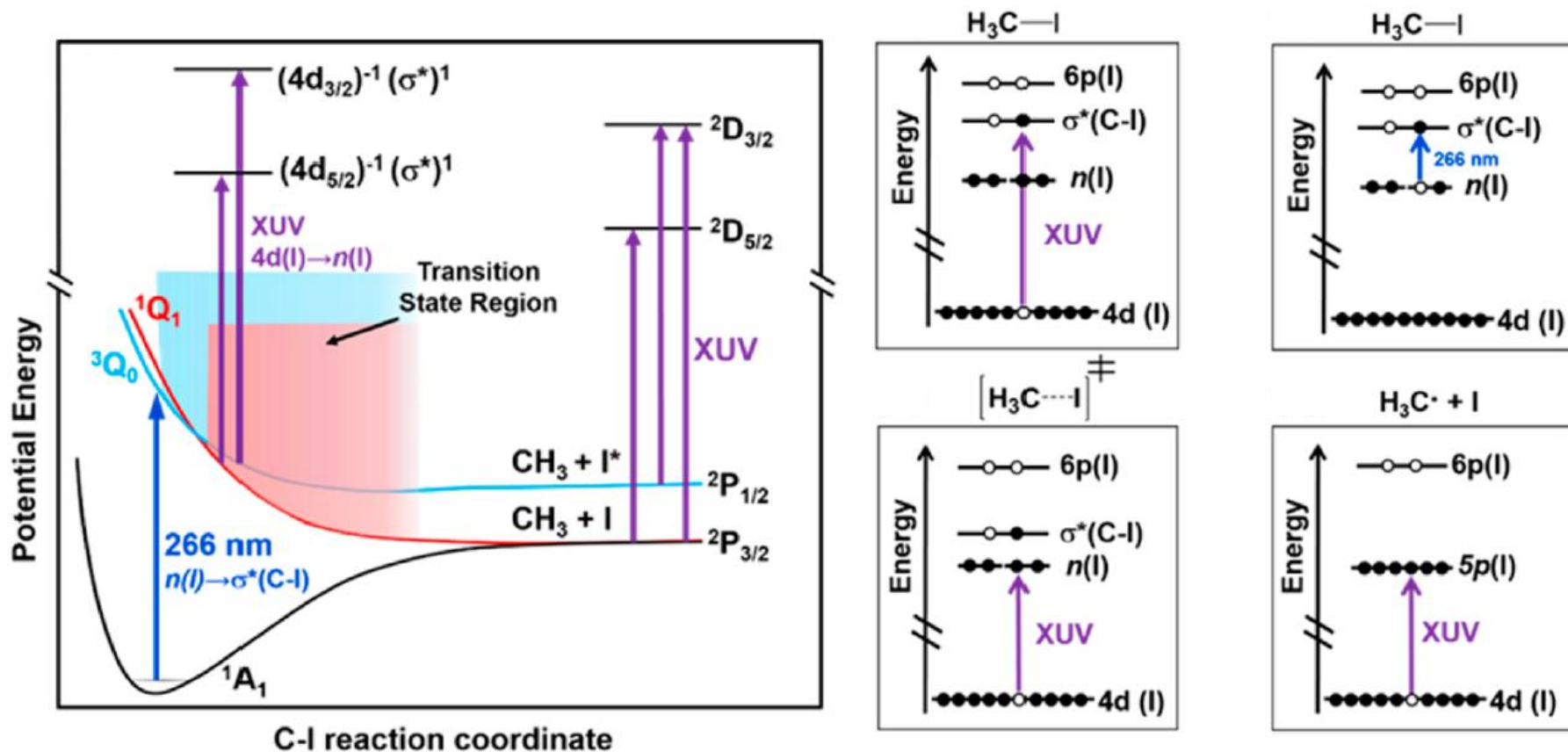


Data analysis software available at www.bristoldynamics.com

M.P. Grubb *et al.*,
Nat. Chem. **8**, 1042 (2016)

3.6 Transient XUV absorption spectroscopy: CH₃I photodissociation

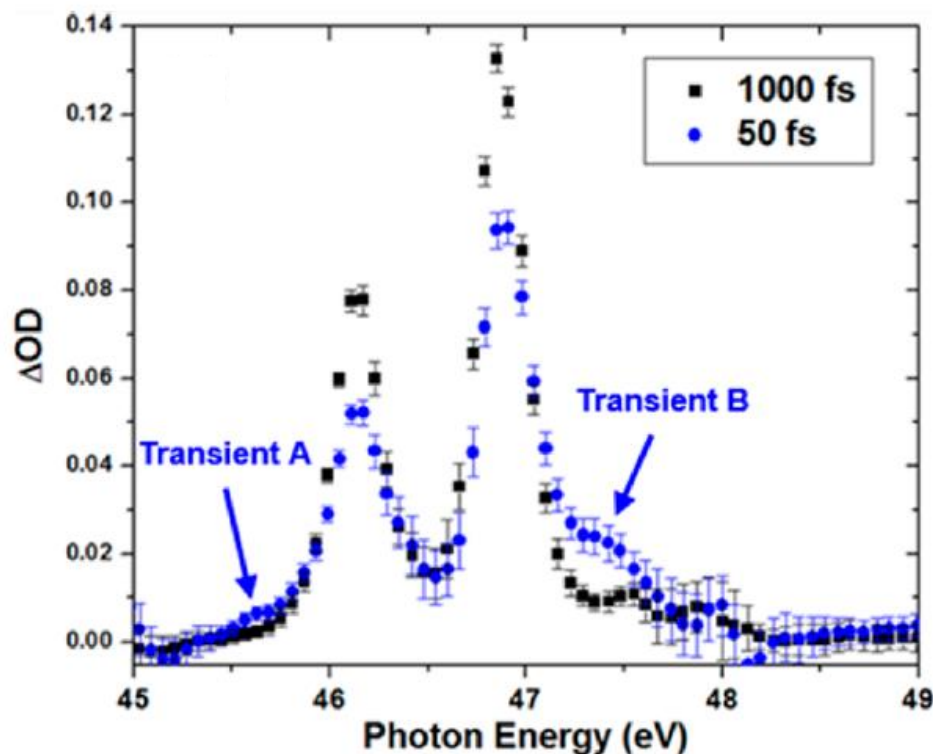
- UV photolysis pulse at 266 nm: $n(\text{I}) \rightarrow \sigma^*(\text{C-I})$ excitation to $^3\text{Q}_0$ and $^1\text{Q}_1$ states
- 35-fs XUV probe pulse (by HHG): 4d core-to-valence excitation on Iodine atom
- Transient absorption spectroscopy (measure ΔOD).



Attar *et al.* JPCLet **6**, 5072 (2015)

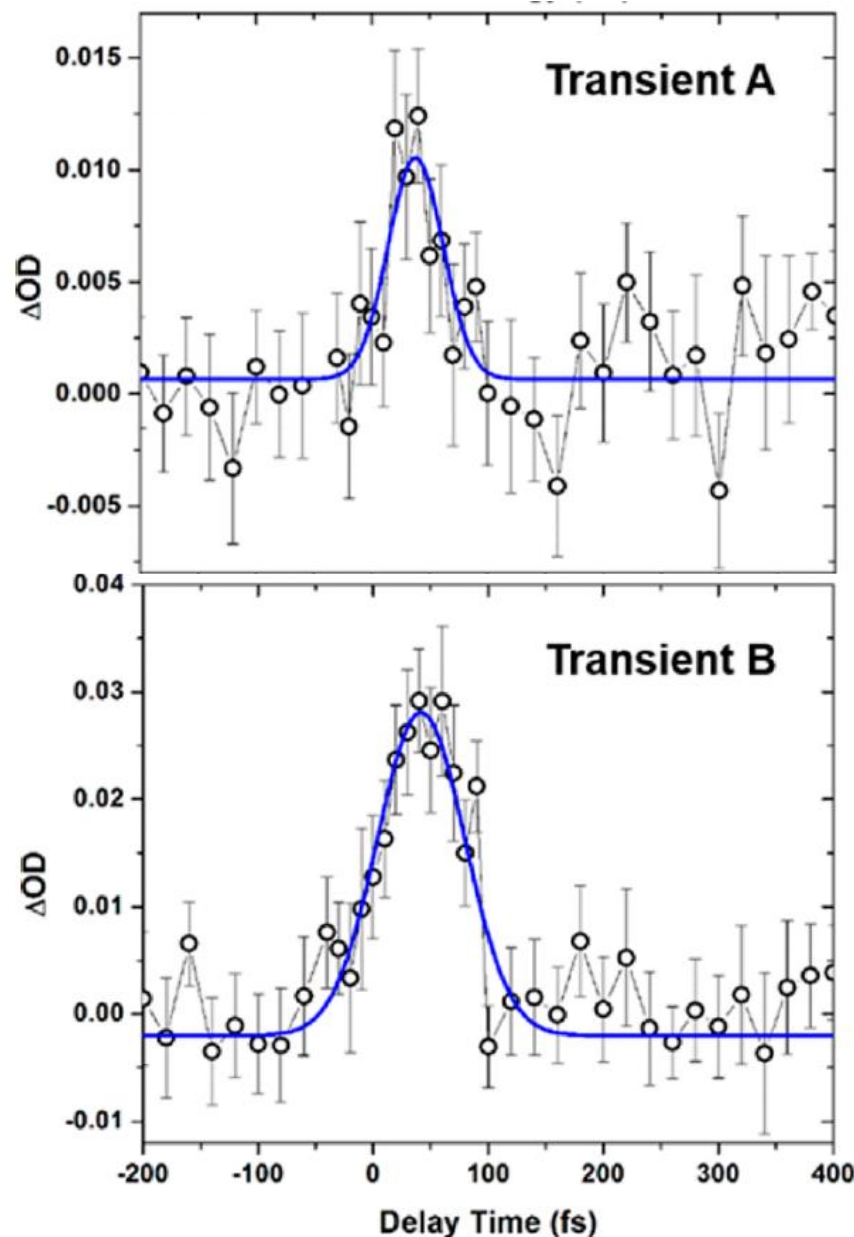
Bhattacharjee *et al.*, J. Chem. Phys. **144**, 124311 (2016)

CH₃I photodissociation: observation of dissociating intermediates on the ³Q₀ and ¹Q₁ states.



Intermediates rise in ~40 fs and decay by 90 fs as bond breaking is complete.

Core excitation gives atom / element specific detection.

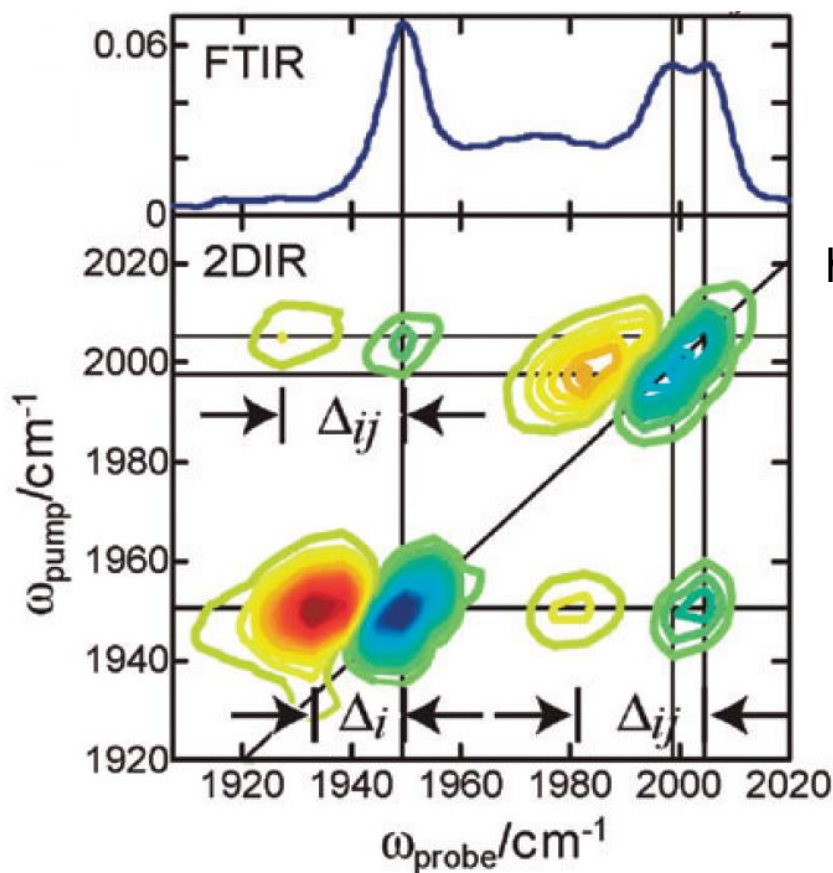
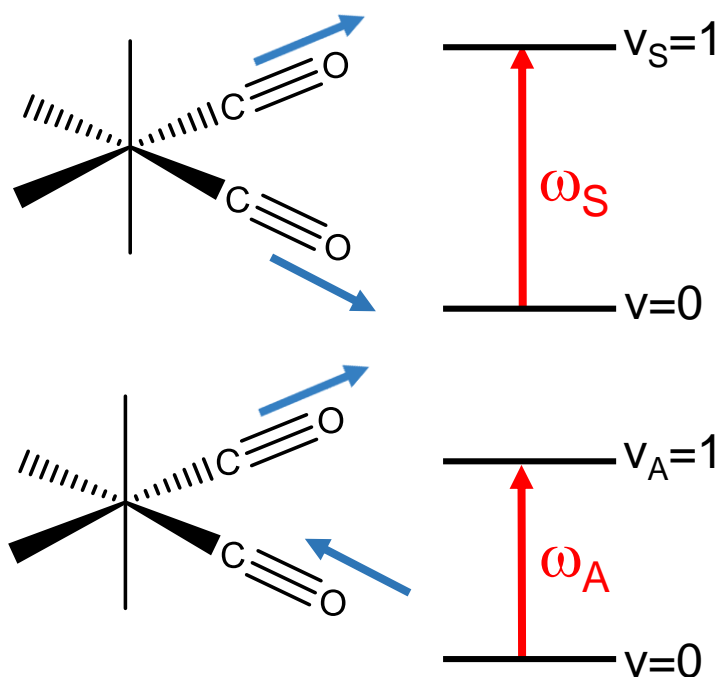


4.0 Two-dimensional spectroscopy

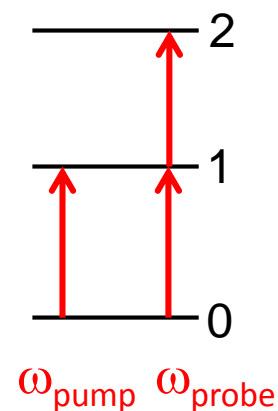
4.1 Principles of 2D Optical Spectroscopy

The principles of 2D spectroscopy methods are illustrated for 2DIR. Examples show how 2DIR can probe relaxation and exchange dynamics in molecules.

Consider a molecule with two vibrational modes:



Each feature has two parts:

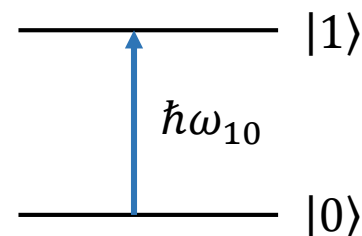


4.2 Density matrix formalism for spectroscopy of molecular systems

What is the effect of a laser pulse on a two-level system? We will develop a 2DIR *response function* treatment for an ensemble of molecules.

The dipolar interaction of the laser field with a molecule is

$$\hat{h}(t) = -\hat{\mu} \cdot \hat{E}(t) = -\hat{\mu} \cdot \hat{E}_0 \cos \omega t$$



After the laser pulse, the molecule is in a linear combination of eigenstates:

$$|\psi(t)\rangle = c_0 e^{-iE_0 t/\hbar} |0\rangle + c_1 e^{-iE_1 t/\hbar} |1\rangle$$

The c_n coefficients contain the transition dipole moments, but are time-independent because the laser pulse is now off.

The coherent superposition $|\psi(t)\rangle$ corresponds to a wavepacket. An ensemble of molecules cannot be described by a single wavefunction. Instead, the time-dependence of this ensemble is called the **molecular response**, $R(t)$.

In an ensemble of molecules we create a **macroscopic polarization** $P(t)$ because the molecules are all driven by the same laser pulse and are initially oscillating in phase.

$P(t)$ is obtained from the molecular response function by convoluting with the electric field of the laser pulse(s).

$$P(t) = \int_0^\infty dt_1 E(t - t_1) R(t_1)$$

For an ultrafast pulse, we can make the approximation $P(t) \propto R(t)$.

For one molecule the response is the expectation value of the transition dipole operator:

$$R(t) = \langle \hat{\mu} \rangle = \langle \psi(t) | \hat{\mu} | \psi(t) \rangle \propto \mu_{10}^2 \sin(\omega_{10} t)$$

The resulting polarization oscillates and emits radiation at ω_{10} with a 90° phase shift. A Fourier transform of the emitted time-dependent field gives the absorption spectrum.

In an ensemble of molecules in different environments, the frequencies of oscillation differ. The oscillations lose their phase relationship and the macroscopic polarization decays to zero over time. In the signal, we observe a Free Induction Decay (FID).

For an ensemble we use a **density matrix** rather than a wavefunction description.

$$\rho = \begin{pmatrix} \rho_{00} & \rho_{01} \\ \rho_{10} & \rho_{11} \end{pmatrix} = \begin{pmatrix} \langle c_0 c_0^* \rangle & \langle -c_0 c_1^* e^{i\omega_{10}t} \rangle \\ \langle c_1 c_0^* e^{-i\omega_{10}t} \rangle & \langle c_1 c_1^* \rangle \end{pmatrix} \quad \langle \dots \rangle \text{ denotes an ensemble average.}$$

Population relaxation and dephasing (e.g. by environmental fluctuations changing the frequencies and hence phases of the individual wavefunctions) contribute time-dependence to the c_n coefficients.

Diagonal elements ρ_{00} and ρ_{11} describe the populations of the states $|0\rangle$ and $|1\rangle$.

Non-zero off-diagonal elements ρ_{10} and ρ_{01} describe coherences.

The coherences decay with dephasing time T_2 , e.g. $\rho_{10}(t) = \rho_{10}(t=0) e^{-t/T_2}$

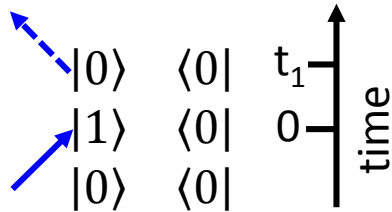
The excited population decays with relaxation time T_1 : $\rho_{11}(t) = \rho_{11}(t=0) e^{-t/T_1}$

Double-sided Feynman diagrams keep track of the interactions of the laser with the molecular ensemble. They represent the matrix elements of the density operator:

$$\hat{\rho}_{mn} = \langle c_m c_n^* \rangle |m\rangle \langle n|$$

$m = n$ are populations

$m \neq n$ are coherences



- Excitation pulse creates a coherence
- Coherence radiates at the same frequency (with 90° phase shift)
- Interference of the two fields gives absorption signal

Response function is: $R^{(1)}(t_1) \propto i\mu_{10}^2 e^{-i\omega_{10}t_1} e^{-t_1/T_2}$

Macroscopic polarization is: $P^{(1)}(t) = \int_0^\infty dt_1 E(t - t_1) R^{(1)}(t_1)$

FID signal is: $E_{sig}^{(1)} \propto i P^{(1)}(t)$ where the factor of i is for a 90° phase shift

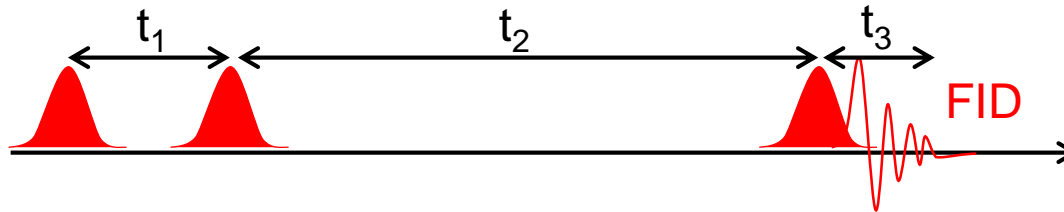
$E_{sig}^{(1)}$ can be measured from its interference with the excitation field.

A Fourier transform gives the spectrum: $S(\omega) \propto \left| \int_0^\infty \{E(t) + E_{sig}^{(1)}(t)\} e^{i\omega t} dt \right|^2$

The outcome is a Lorentzian profile
absorption feature with FWHM = $1/\pi T_2$

$$A(\omega) \propto \mu_{10}^2 \frac{1/T_2}{(\omega - \omega_{10})^2 + 1/T_2^2}$$

Pulse sequences and response functions for 2D spectroscopy:

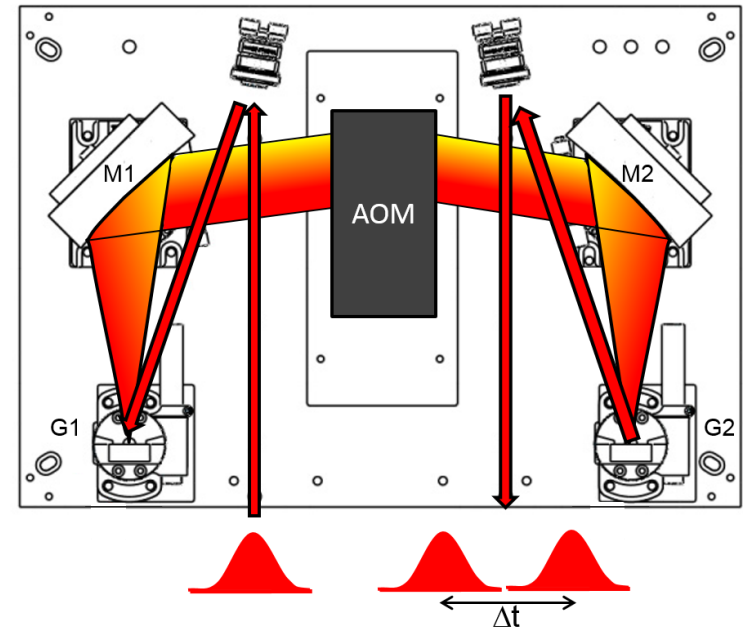


t_1 is the *coherence* time

t_2 is the *population* or *waiting* time

The coherence time can be controlled using a pulse shaper:

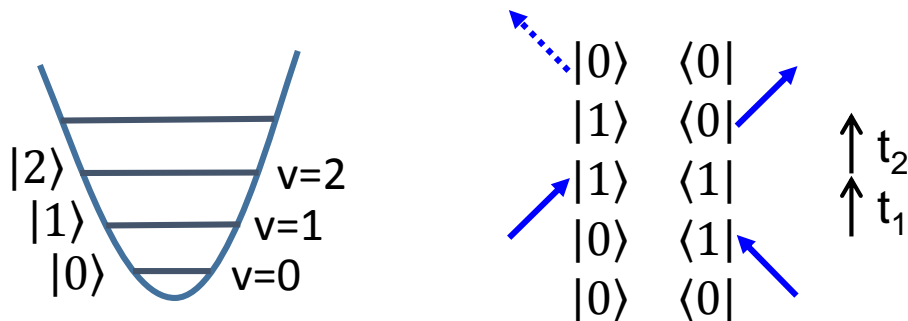
S.H. Shim and M.T. Zanni,
PCCP **11**, 748 (2009)



In the 2D spectrum:

- The first frequency axis is obtained by Fourier transformation over t_1
- The second frequency axis comes from Fourier transformation over t_3 or by dispersing the emitted field in a spectrometer.

Example for a single vibrational mode: One possible Feynman pathway is



Coherence dephasing during t_1 and t_3

$$R^{(3)}(t_1, t_2, t_3) \propto i\mu_{10}^4 e^{i\omega_{10}t_1} e^{-t_1/T_2} e^{-t_2/T_1} e^{-i\omega_{10}t_3} e^{-t_3/T_2}$$

Coherence oscillates at frequency ω_{10} during periods t_1 and t_3

Population relaxation during t_2

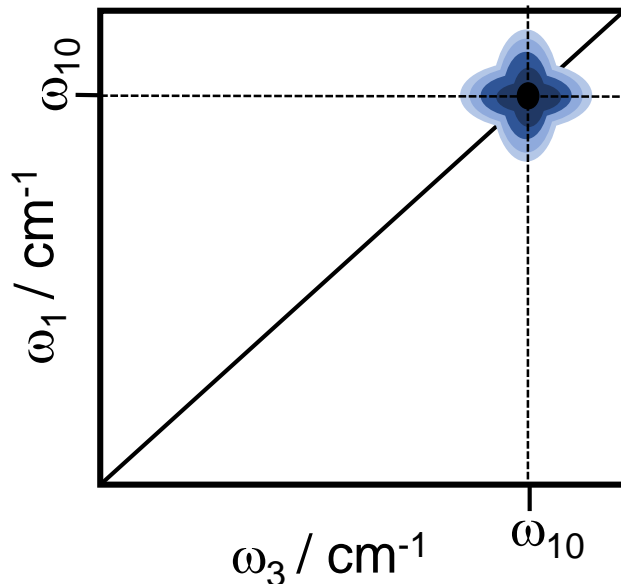
$$S^{(3)}(\omega_1, t_2, \omega_3) \propto \int_0^\infty \int_0^\infty iR^{(3)}(t_1, t_2, t_3) e^{i\omega_3 t_3} e^{i\omega_1 t_1} dt_1 dt_3$$

We obtain a time-dependent 2D spectrum from:

$$S^{(3)}(\omega_1, t_2, \omega_3) \propto \int_0^\infty \int_0^\infty iR^{(3)}(t_1, t_2, t_3) e^{i\omega_3 t_3} e^{i\omega_1 t_1} dt_1 dt_3$$

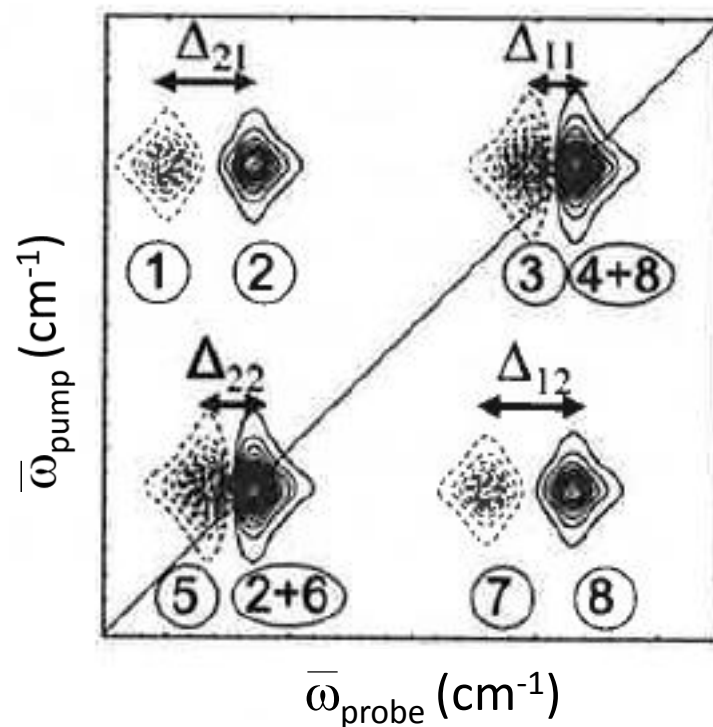
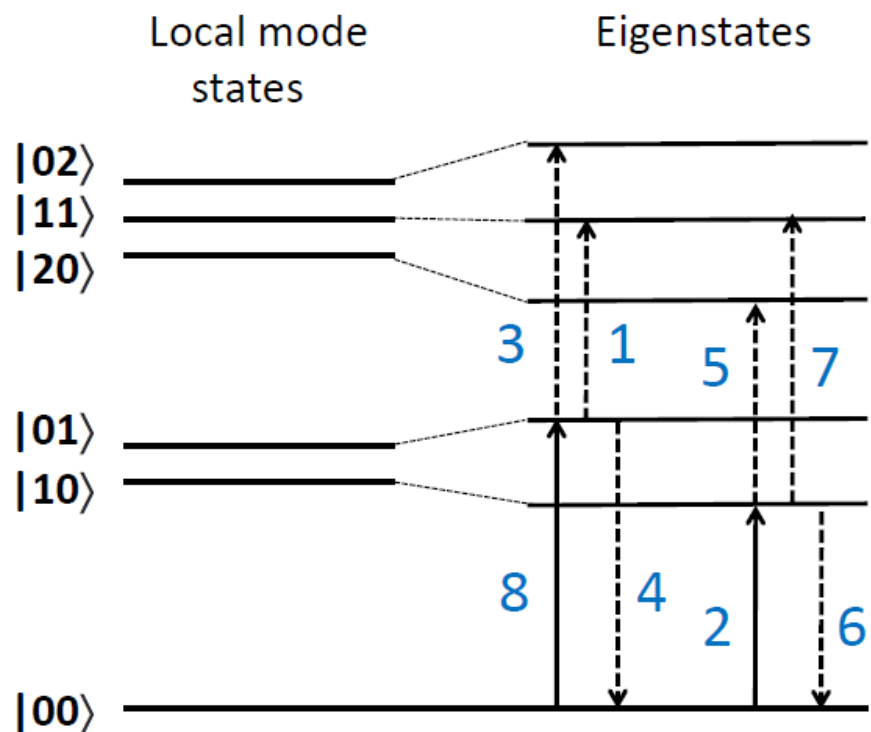
$$S^{(3)}(\omega_1, t_2, \omega_3) = \frac{1}{i(\omega_1 - \omega_{10}) - 1/T_2} \cdot \frac{1}{i(\omega_3 - \omega_{10}) - 1/T_2}$$

Combining the signal fields for different pathways to make an absorptive spectrum gives a double-Lorentzian 2D lineshape:



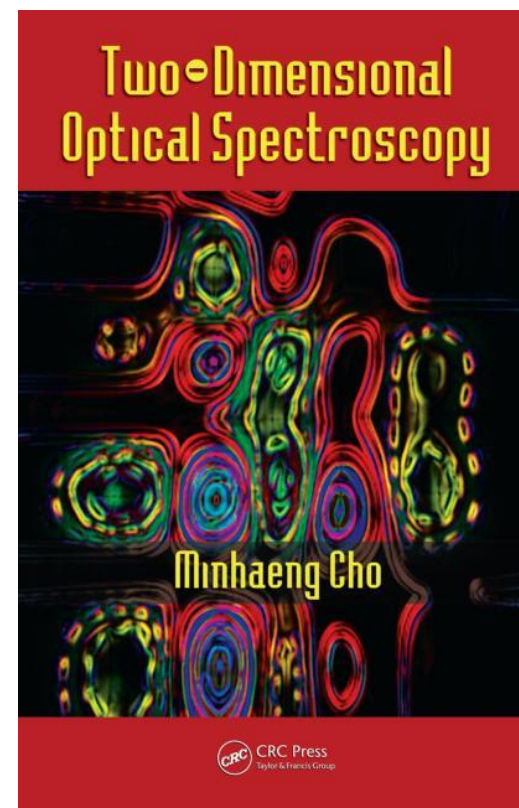
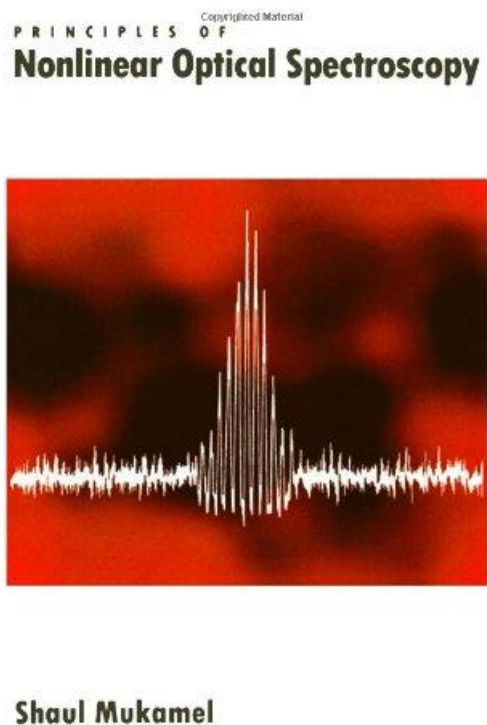
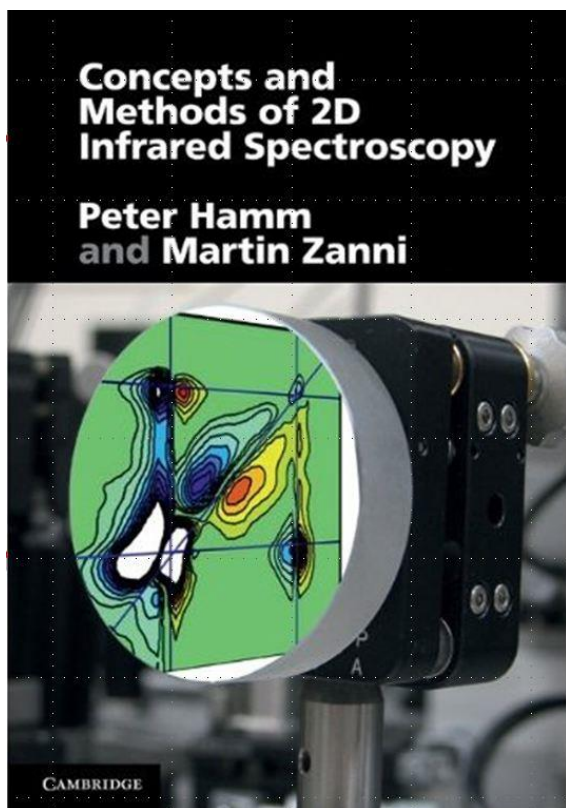
Different Feynman pathways give rise to other features in the 2DIR spectrum, e.g. those involving excitation from $|1\rangle$ to $|2\rangle$.

Transitions that contribute to a typical 2DIR spectrum of two coupled oscillators

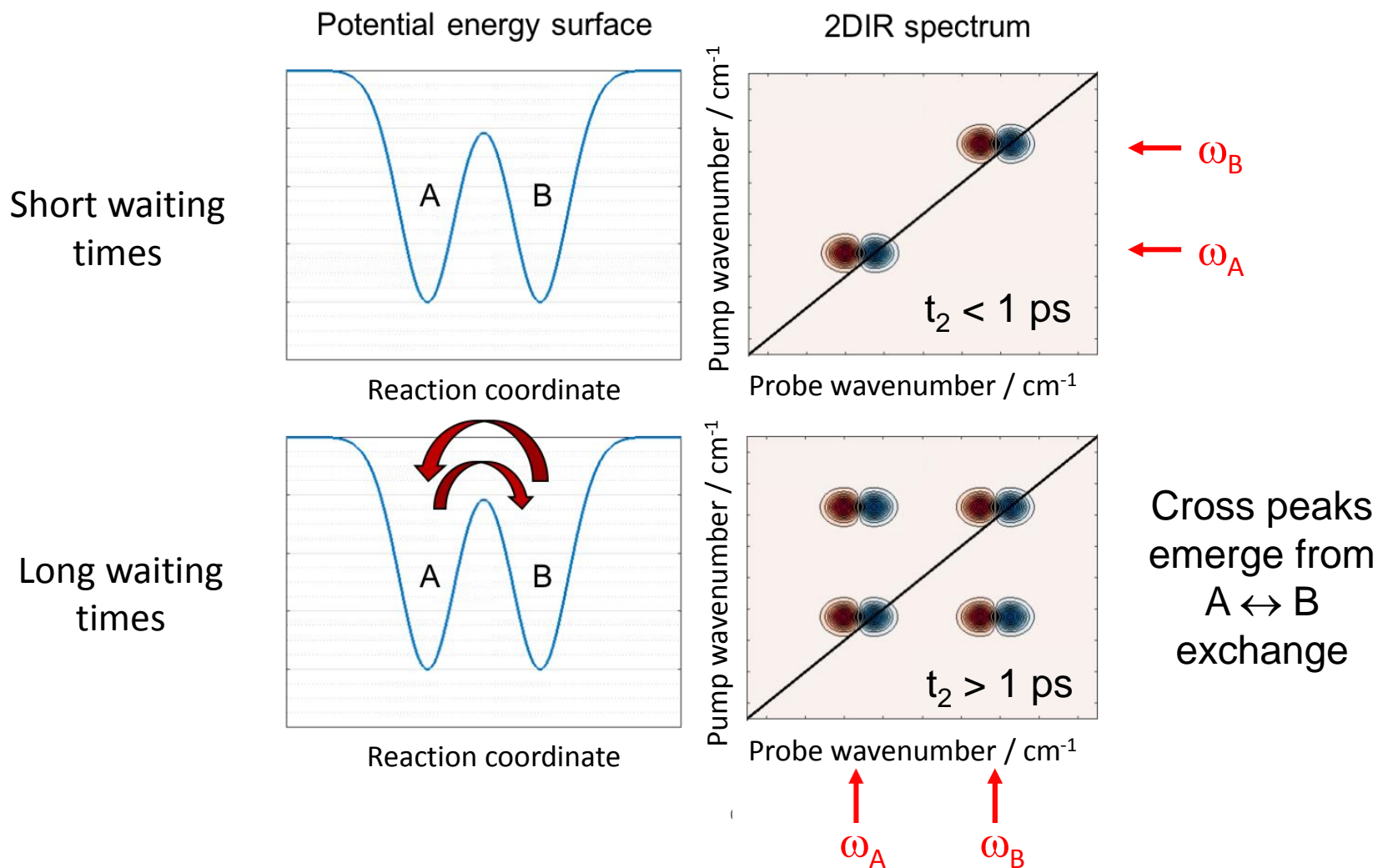


Δ_{ij} are diagonal ($i = j$) and off-diagonal ($i \neq j$) anharmonic shifts.

Further reading on 2D spectroscopy:



4.3 Chemical exchange observed by 2DIR



5.0 Spectral simulation using the PGOPHER program

PGOPHER is a program for simulating and fitting rotational, vibrational and electronic spectra of molecules.

The program can be downloaded free from <http://pgopher.chm.bris.ac.uk/>

It is written and maintained by Dr Colin Western and a recent publication describes its use and the underlying theory:

C.M. Western, J. Quant. Spectrosc. Radiat. Trans. **186**, 221 (2016).

Guidance can be obtained from the PGOPHER website.

6.0 Conclusions

Spectroscopic methods with high frequency or time resolution provide incisive observations of the dynamics of photochemical and chemical reactions.

These observations can be compared to the predictions of computational studies to provide rigorous tests of theories of chemical dynamics.

The Chemical Dynamics community has the spectroscopic tools available to impact on mechanistic understanding in other disciplines such as synthetic chemistry, biochemistry, combustion science, solar energy capture, plasma processing, astrochemistry and atmospheric chemistry.

Advances in spectroscopic techniques, and access to major facilities such as synchrotrons and free electron lasers, continue to reveal new and exciting dynamical information.